

Magneto-optical study of Li and Na acceptor bound excitons in CdTe: Fine structure and cubic crystal-field effect

E. Molva*

*Département de Recherche Fondamentale, Section de Physique du Solide,
Centre d'études nucléaires de Grenoble, 85X, 38041 Grenoble Cedex, France*

Le Si Dang

*Laboratoire de spectrométrie physique, Université Scientifique et Médicale de Grenoble,
Boîte Postale 87, 38402 Saint Martin d'Hères Cedex, France*

(Received 20 June 1984; revised manuscript received 2 January 1985)

We present a high-resolution optical study of Li and Na shallow-acceptor bound excitons in CdTe. Results of absorption and Zeeman-effect experiments on the photoluminescence are discussed in terms of the j - j coupling scheme in cubic symmetry. It is shown that (i) the low-lying bound-exciton states are derived from the $J=2$ two-hole state, and (ii) the cubic crystal-field effect is dominant over the electron-hole interaction. The magnetic parameter values are the same as those previously determined for the Cu and Ag deeper-acceptor bound excitons: $g_e = -1.77$ for the electron, $K = +0.61$, and $L = -0.04$ for the hole.

I. INTRODUCTION

Low-lying excited states of acceptor bound excitons (BE) have been observed in various direct-gap semiconductors with the zinc-blende-type structure.¹ The origin of this fine structure is usually attributed to exchange interactions between the bound particles, namely, two Γ_8 holes with angular momentum $j = \frac{3}{2}$, and one Γ_6 electron with angular momentum $j = \frac{1}{2}$. In the j - j coupling scheme,¹ the two Γ_8 holes are combined antisymmetrically to form $J=0$ (Γ_1) and $J=2$ ($\Gamma_3 + \Gamma_5$) states. Then additional coupling to the Γ_6 electron would yield four BE states with fictitious total angular momentum $K = \frac{1}{2}$ (Γ_6), $K = \frac{3}{2}$ (Γ_8), $K = \frac{1}{2}$ (Γ_7), and $K = \frac{3}{2}$ (Γ_8) since $\Gamma_1 \times \Gamma_6 = \Gamma_6$, $\Gamma_3 \times \Gamma_6 = \Gamma_8$, $\Gamma_5 \times \Gamma_6 = \Gamma_7 + \Gamma_8$ in the T_d point group. The level ordering of these BE states has been discussed by several authors.²⁻⁵ Experimentally, BE states deriving from the $J=2$ two-hole state appear to be the lowest energy for shallow acceptors,⁶⁻⁸ while just the opposite situation is true for deeper acceptors.⁹⁻¹³

In this paper we investigate the fine structure of acceptor BE in CdTe. CdTe is a cubic semiconductor with a direct gap $E_g = 1.606$ eV at $T = 4.2$ K. The nature of acceptor impurities has been recently examined by systematic backdoping experiments correlated with photoluminescence (PL), infrared absorption, and electrical measurements.¹⁴⁻¹⁷ It is found that Cu, Ag, Li, and Na are the main acceptors in high-purity p -type CdTe. Their binding energies are $E_A = 146$ meV (Cu), 107.5 meV (Ag), 58.0 meV (Li), and 58.6 meV (Na), to be compared with the effective-mass value of ~ 57 meV. Thus Cu and Ag are deep acceptors with large attractive central-cell corrections, by contrast to Li and Na acceptors which are more effective-mass-like. Absorption and Zeeman effects on the PL of these acceptor BE have been measured. The results clearly show that the level ordering of BE states is

inverted when going from deep to shallow acceptors. The BE ground states are derived from the $J=0$ two-hole state for Cu and Ag,¹³ and from the $J=2$ two-hole state for Li and Na. More interesting is the fact that the cubic crystal field is found to be dominant over the electron-hole interaction. In the case of Li and Na BE, the crystal-field effect is such that the $J=2$ two-hole state is split into a fundamental Γ_3 doublet and an excited Γ_5 triplet. Thus the low-lying BE states are a Γ_8 ground state and nearly degenerated Γ_7, Γ_8 excited states. This situation is very similar to that observed for shallow-acceptor BE in GaAs (Ref. 7) and InP (Ref. 8).

II. EXPERIMENTAL

Single crystals of CdTe were grown by B. Schaub [Laboratoire d'Electronique et de Technologie de l'Informatique (LETI)—Grenoble] using a modified Bridgman method. They were high-purity p type, with uncompensated acceptor concentrations of $\sim 5 \times 10^{14}$ cm⁻³. The residual acceptors are Li, Na, Ag, and Cu, the latter being always the dominant acceptor in our samples.¹⁴⁻¹⁷ Higher doping levels can be easily obtained by diffusion.¹⁵⁻¹⁸ For Li and Na diffusions, a nitrate solution is deposited on the clean surface of an undoped sample. Then diffusion is performed in a lamp furnace at low temperatures (300°C–600°C) for about 1 h and under a flow of H₂-N₂ gas mixture. Samples prepared with this process contain Li or Na concentrations up to $\sim 10^{17}$ cm⁻³ as given by electrical measurements made on Schottky diodes.

Most optical measurements were performed with the samples immersed in liquid helium pumped below the λ point ($T \sim 1.8$ K). Optical transmission spectra were recorded using a tungsten light source. The samples were thinned to ~ 25 μ m by polishing and etching in a

Br-methanol solution.

PL was excited with the 4880-Å line of an Ar⁺ laser. Typical excitation power of ~10 mW was used, the laser beam being either unfocused or focused on a spot diameter of ~0.2–0.3 mm. The PL was analyzed by a grating monochromator (THR—Jobin Yvon) and detected with a photomultiplier. The spectral resolution was set to ~0.02 meV.

Zeeman spectroscopy was carried out in both Faraday and Voigt configurations, with the magnetic field directed along one of the main crystallographic directions (100) and (111). Magnetic fields up to 45 kG were produced by a split-coil superconducting magnet. The samples were carefully etched before each run. This is to remove inadvertent built-in strains on sample surfaces which can quite often induce significant splittings of BE lines.¹⁹ To avoid depolarization effects, the PL was always collected perpendicularly to the excited face of the sample.

III. ABSORPTION AND PHOTOLUMINESCENCE MEASUREMENTS

A. Cu and Ag bound excitons

Figure 1(a) shows the typical transmission spectrum in the exciton region of an undoped *p*-type sample. The residual acceptor impurities are Cu and Ag in concentrations of $\sim 5 \times 10^{14} \text{ cm}^{-3}$. Their absorptions are denoted A_{11}^{Cu} and A_{11}^{Ag} in the figure. The other absorption features on the high-energy side of the spectrum are due to ionized donor BE (D^+X); neutral donor-free hole transition (D^0, h); neutral donor BE (D_1^1, D_2^2, D_3^3), and free-exciton (FE).²⁰ Note the large oscillator strength of donor-related transitions as compared to that of acceptor transitions. This is remarkable because of the very low donor concentration in these high-purity *p*-type samples. Such observation has been also reported for ZnTe.^{21,22}

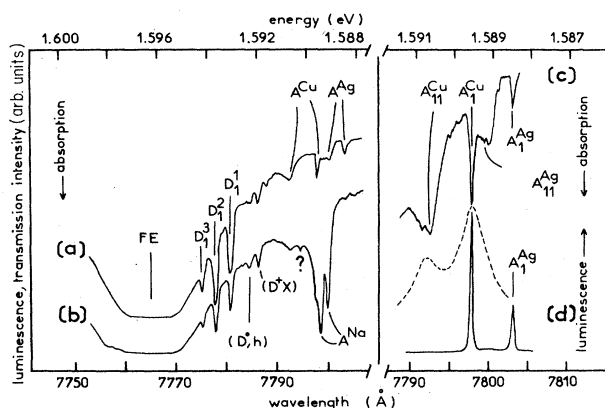


FIG. 1. (a) Transmission spectrum of a high-purity *p*-type CdTe ($N_A - N_D = 5 \times 10^{14} \text{ cm}^{-3}$) at $T = 1.8 \text{ K}$. A_{11}^{Cu} and A_{11}^{Ag} are absorptions due to Cu and Ag BE, respectively. (b) Transmission spectrum of a Na-doped sample ($N_A - N_D = 10^{16} \text{ cm}^{-3}$) at $T = 1.8 \text{ K}$. A_{11}^{Na} is absorption due to Na BE. (c) Same as (a). (d) Photoluminescence of a high-purity *p*-type CdTe ($N_A - N_D = 5 \times 10^{14} \text{ cm}^{-3}$) at $T = 1.8 \text{ K}$ (solid curve) and 7 K (dashed curve). Thermalization effects between the Cu BE states are clearly observed by comparison of (c) and (d).

Details of Cu and Ag BE absorption are shown in Fig. 1(c). The sharp peaks A_{11}^{Cu} at 1.5896 eV and A_{11}^{Ag} at 1.5885 eV have been attributed to Cu and Ag BE ground states, respectively. A second broad peak, labeled A_{11}^{Cu} , appears at ~1.2 meV above A_{11}^{Cu} . It corresponds to Cu BE excited states, as evidenced by thermalization effects between A_{11}^{Cu} and A_{11}^{Cu} observed in the PL spectra at $T = 1.8$ and 7 K [see Fig. 1(d)]. Similarly, there is a second broad peak, labeled A_{11}^{Ag} , at ~0.7 meV above A_{11}^{Ag} .

Recent Zeeman spectroscopy on the PL of A_{11}^{Cu} and A_{11}^{Ag} has shown that both lines correspond to the Γ_6 ($K = \frac{1}{2}$) BE ground state.¹³ This is a quite common situation for deep-acceptor BE.⁹⁻¹² According to Herbert,³ the $J = 0$ two-hole state is more sensitive to hole attractive central-cell corrections than the $J = 2$ two-hole state. Therefore, the $J = 0$ state can be pulled below the $J = 2$ state for sufficiently deep acceptors, and one obtains the sequence of $K = \frac{1}{2}, \frac{3}{2}, \frac{5}{2}$ BE states in order of increasing energy. The predicted relative oscillator strengths of $K = \frac{1}{2}, \frac{3}{2}, \frac{5}{2}$ BE states and $K = \frac{1}{2}$ BE state are 5:1. This ratio is very close to the measured absorption intensity of the two Cu and Ag BE states: $A_{11}^{\text{Cu}}:A_{11}^{\text{Ag}} \sim 4:1$, and $A_{11}^{\text{Ag}}:A_{11}^{\text{Cu}} \sim 5:1$. Thus it is tempting to assign the broad A_{11}^{Cu} and A_{11}^{Ag} lines to unresolved $K = \frac{3}{2}, \frac{5}{2}$ BE state of Cu and Ag, respectively. If this is correct, then the hole-hole splitting will be ~1.2 meV for Cu BE and ~0.7 meV for Ag BE.

B. Li and Na bound excitons

Figure 1(b) shows the transmission spectrum of a Na-doped sample, with the concentration ($N_A - N_D$) $\sim 10^{16}$

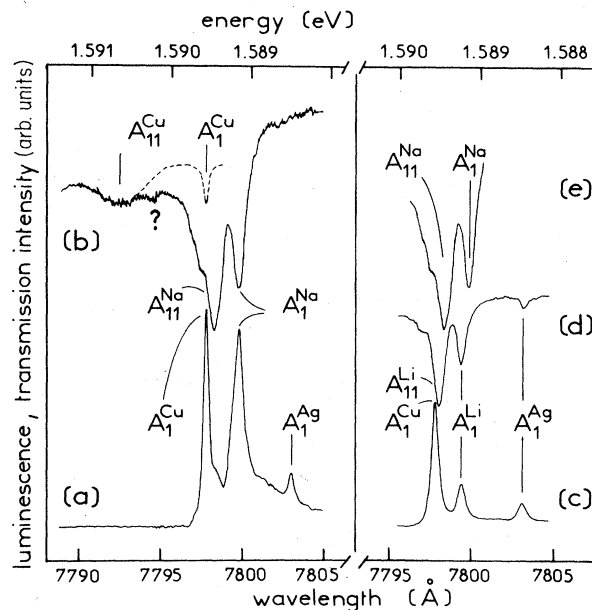


FIG. 2. Details of absorption and photoluminescence at $T = 1.8 \text{ K}$ of acceptor BE. CdTe: Na ($N_A - N_D = 10^{16} \text{ cm}^{-3}$); (a) photoluminescence, (b) and (e) absorption. The dotted curve represents, approximately, absorptions due to Cu BE. CdTe: Li ($N_A - N_D = 10^{15} \text{ cm}^{-3}$); (c) photoluminescence, (d) absorption. Note that the fine structure is the same for Li and Na BE.

cm^{-3} . We observe two strong absorption lines at 1.589 16 and 1.589 47 eV labeled A^{Na} (labeled A_1^{Na} and A_{11}^{Na} , respectively, in Fig. 2). Absorption from Cu and Ag acceptors is rather weak since their concentrations are about the same as in undoped samples ($5 \times 10^{14} \text{ cm}^{-3}$). The relative oscillator strengths between the two Na lines are in the ratio $A_{11}^{\text{Na}}:A_1^{\text{Na}} \sim 1.9:1$. However, the A_1^{Na} low-energy line is much stronger in emission (see Fig. 2), indicating that the A_1^{Na} and A_{11}^{Na} lines correspond to the ground and excited BE states, respectively. Similar absorption and emission features are observed in Li-doped samples. The two Li BE lines are A_1^{Li} at 1.589 23 eV and A_{11}^{Li} at 1.589 51 eV (see Fig. 2).

From the Zeeman study of A_1^{Li} and A_{11}^{Na} lines given in the next section, we conclude that Li and Na BE states are derived from the $J=2$ two-hole state. Therefore, these BE states can be described by the following effective Hamiltonian:

$$H_0 = b\mathbf{J} \cdot \mathbf{j} + V_c, \quad (1)$$

where $J=2$, $j=\frac{1}{2}$. b is a parameter defining the strength of the (isotropic) electron-hole interaction. V_c represents the effect of the T_d crystal field. Its matrix representation in the $|J=2, M_J\rangle$ basis will be written as the following (the matrix elements are taken from Ref. 23):

$$V_c = c \begin{pmatrix} | +2 \rangle & | +1 \rangle & | 0 \rangle & | -1 \rangle & | -2 \rangle \\ \hline \frac{1}{4} & 0 & 0 & 0 & \frac{5}{4} \\ 0 & -1 & 0 & 0 & 0 \\ 0 & 0 & \frac{3}{2} & 0 & 0 \\ 0 & 0 & 0 & -1 & 0 \\ \frac{5}{4} & 0 & 0 & 0 & \frac{1}{4} \end{pmatrix} \begin{pmatrix} | +2 \rangle \\ | +1 \rangle \\ | 0 \rangle \\ | -1 \rangle \\ | -2 \rangle \end{pmatrix}, \quad (2)$$

where c is the crystal-field parameter. From the form of the electron-hole interaction in (1) and the crystal field V_c in (2), it is easy to see that these two interactions are of equal strength for $|b| = |c|$. Solutions of (1) are straightforward for the two limiting situations: $|b| \ll |c|$ and $|b| \gg |c|$. In the first situation ($|b| \ll |c|$), the cubic field splits the $J=2$ state into a Γ_3 doublet and a Γ_5 triplet with an energy splitting equal to $\frac{5}{2}c$. The BE states are a Γ_8 state and degenerated ($\Gamma_7 + \Gamma_8$) states with oscillator strengths in the ratio 2:3.²⁴ The opposite situation ($|b| \gg |c|$) corresponds to the spherical symmetry, and the BE states are $D_{3/2}$ and $D_{5/2}$ states separated by $\frac{5}{2}b$. Their oscillator strengths are in the ratio 4:1.^{25,24} For the more general situation ($b \neq 0, c \neq 0$), numerical computations are necessary to get the BE energies and their oscillator strengths. The result is schematically shown in Fig. 3. The numbers in parentheses represent the relative oscillator strengths of BE states. Note that the oscillator strength of the Γ_7 BE state is independent of b and c , and equal to $\frac{1}{3}$.⁷ On the other hand, the oscillator strengths of the two Γ_8 BE states depend on the relative magnitude of b and c since these states are mixed by the electron-hole interaction and the cubic field.

We have used (1) to fit the absorption data. Two conclusions can be drawn: (i) the crystal-field term is dominant over the electron-hole interaction, and (ii) the crystal-field parameter c is negative. In fact, best fits to the Zeeman data are obtained for $b \sim -0.01$ meV, $c \sim -0.11$ meV (see Sec. IV). Computing (1) with this set of parameter values, we obtain nearly degenerate Γ_7, Γ_8 BE states at ~ 0.28 meV above a Γ_8 BE ground state, their oscillator strengths being in the ratio $\sim 1.7:1$. These results are in good agreement with the absorption data in Fig. 2.

To summarize, the low-lying BE states of Li and Na acceptors are derived from the $J=2$ two-hole state. The cubic crystal field ($c \sim -0.11$ meV) is dominant over the electron-hole interaction ($b \sim -0.01$ meV) so that the $J=2$ state first splits into a ground Γ_3 doublet and an excited Γ_5 triplet. Then coupling to the Γ_6 electron yields BE states of Γ_8, Γ_7 , and Γ_8 symmetry in order of increasing energy. We assign the $A_1^{\text{Li,Na}}$ and $A_{11}^{\text{Li,Na}}$ lines to the Γ_8 and $(\Gamma_7 + \Gamma_8)$ BE states, respectively. The latter two states are nearly degenerate because of the smallness of the electron-hole interaction. It is interesting to note that a similar level ordering has been observed for shallow-acceptor BE in GaAs (Ref. 7) and InP (Ref. 8). Also the cubic-crystal-field splitting (~ 0.3 meV) is comparable to that measured for acceptor BE in GaAs (Ref. 7) (~ 0.18 meV), InP (Ref. 8) (~ 0.23 meV), Si (Ref. 24) (~ 0.3 – 0.4 meV), or for an exciton bound to isoelectronic Bi traps in GaP (Ref. 26) (~ 0.28 meV). We do not know the magnitude of the hole-hole interaction for Li and Na BE. This is because no absorption (or emission) line can be definitely attributed to the Γ_6 ($K=\frac{1}{2}$) BE state, although the transmission spectrum of Na-doped samples exhibits a small unidentified absorption peak [marked in Figs. 1(b) and 2(b)] at ~ 1 meV above the A_1^{Na} line. However, no such feature is observed in Li-doped samples.

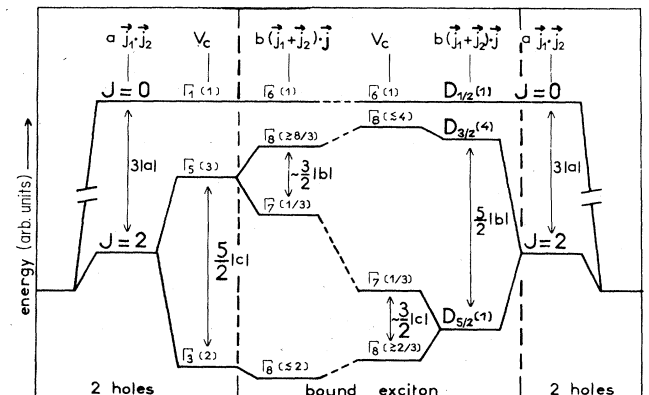


FIG. 3. Diagram showing the fine structure of acceptor BE in cubic semiconductors as a function of the hole-hole interaction (a), the electron-hole interaction (b), and the cubic crystal field (V_c). The parameters a , b , and c (V_c) are assumed to be negative $j_1 = j_2 = \frac{3}{2}$ (hole), $j = \frac{1}{2}$ (electron). Numbers in parentheses represent the relative oscillator strengths (see text).

IV. ZEEMAN EFFECTS

A. Experimental results

In this section we present Zeeman effects on the PL spectra of Li- and Na-doped samples. The doping levels are rather low ($\leq 10^{15} \text{ cm}^{-3}$) to avoid any broadening of BE lines. So the samples used in these experiments contain an important amount of Cu ($\sim 5 \times 10^{14} \text{ cm}^{-3}$) and Ag in addition to the diffused impurity Li or Na.

Figure 4 shows the PL spectra in magnetic fields of a Li- and Na-diffused sample. The Cu and Ag lines are easily identified from previous studies.¹³ The other lines are due to Li and Na BE. Their behaviors in magnetic fields are the same within our experimental conditions. There is just a small energy shift of $\sim 0.1 \text{ meV}$ which corresponds roughly to the energy difference between the A_1^{Li} and A_1^{Na} lines in zero field. Therefore, we will only discuss the Zeeman data obtained for a Li-doped sample in the following.

Figures 5–7 show the Zeeman spectra recorded with \mathbf{H} parallel to the $\langle 100 \rangle$ and $\langle 111 \rangle$ crystallographic directions in the Faraday configuration (σ_+ , σ_- circular polarizations).

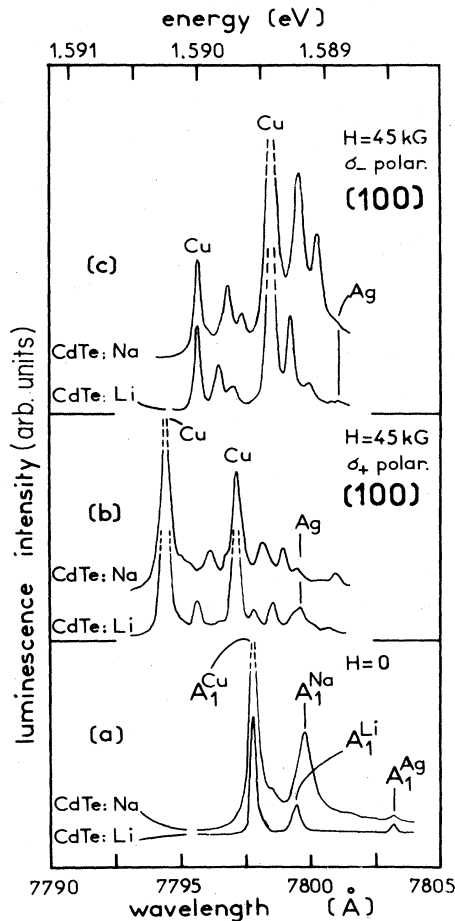


FIG. 4. Comparison of Zeeman spectra obtained for a Li- and a Na-doped CdTe at $T=1.8 \text{ K}$ and or $\mathbf{H} \parallel \langle 100 \rangle$. (a) $H=0$. (b) $H=45 \text{ KG}$ and for σ_+ polarization. (c) Same as (b) but for σ_- polarization. Note the similarity of the Zeeman features for Li and Na BE.

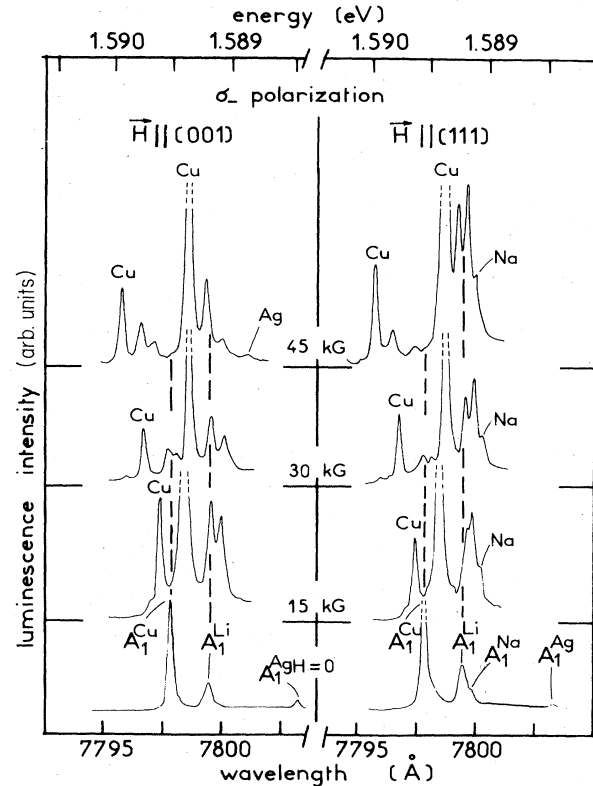


FIG. 5. Zeeman effects observed for a Li-doped CdTe ($N_A - N_D \sim 10^{15} \text{ cm}^{-3}$) for the circular polarization σ_- and $\mathbf{H} \parallel \langle 100 \rangle$ and $\langle 111 \rangle$.

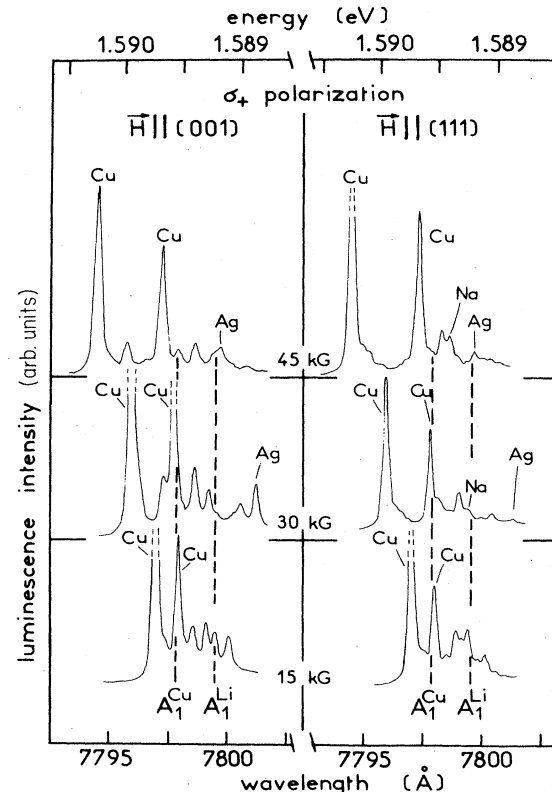
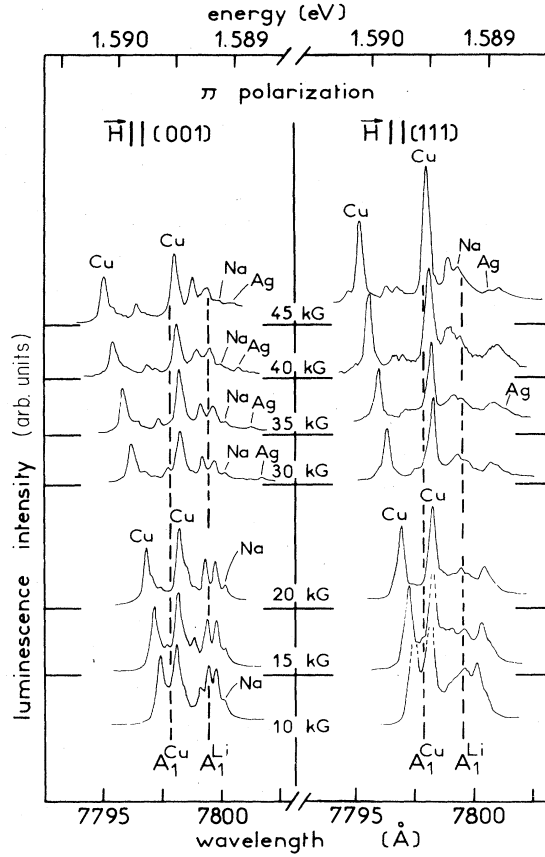


FIG. 6. Same as in Fig. 5 but for the circular polarization σ_+ .

FIG. 7. Same as in Fig. 5 but for the linear polarization π .

zations) and in the Voigt configuration (π linear polarization). Due to the presence of the strong Cu lines, it is not possible to observe the complete Zeeman splittings of the Li BE lines. It is clear, however, that the Zeeman spectra of Li are more complex than those of Cu. For example, the A_1^{Li} line splits into four or more lines for a given polarization σ_+ , σ_- , or π . The anisotropy of the Zeeman spectra is also stronger for Li than for Cu. Fan charts of Zeeman effects are shown in Figs. 8–10. The solid and open circles represent the relative energies of the Li and Cu lines, respectively. Note the existence of diamagnetic effects which tend to shift the lines toward higher energies.⁹ The various solid and dashed curves drawn are the results of the calculations as discussed below.

B. Discussion

The Zeeman data clearly show that the nature of the BE states involved in the recombination process is different for (Li,Na) acceptors and (Cu,Ag) acceptors. In the latter case, the BE ground state is a Γ_6 ($K=\frac{1}{2}$) state which is derived from the $J=0$ two-hole state.¹³ This leads us to assume that the Li and Na BE ground states are derived from the $J=2$ two-hole state. Their energies in magnetic fields can be described by the following effective Hamiltonian:

$$H_{\text{BE}} = H_0 + H_1 + dH^2, \quad (3)$$

$$H_1 = g_e \mu_B \mathbf{H} \cdot \mathbf{j} + K \mu_B \mathbf{H} \cdot (\mathbf{j}_1 + \mathbf{j}_2) + L \mu_B [(j_{1x}^3 + j_{2x}^3) H_x + \dots], \quad (4)$$

where $j = \frac{1}{2}$, $j_1 = j_2 = \frac{3}{2}$. H_0 represents the zero-field Hamiltonian given in (1), H_1 the linear Zeeman effect, and dH^2 the diamagnetic shift.⁹ μ_B is the Bohr magneton, g_e is the electron g factor, K and L are the hole parameters corresponding to the isotropic and anisotropic Zeeman effect in a Γ_8 state, respectively.²⁷

The final state of the recombination process is the acceptor Γ_8 state. The Zeeman effect in this state is given by²⁷

$$H_A = K \mu_B \mathbf{H} \cdot \mathbf{j} + L \mu_B (j_x^3 H_x + \dots) \quad (5)$$

where $j = \frac{3}{2}$. Here we have assumed that (i) the Zeeman effect in the acceptor state is the same as that of the hole in the BE states, (ii) the diamagnetic shift in the acceptor state can be neglected. To simplify the fitting procedure, we further assume that the g_e , K , and L values are those we have already determined for the Cu and Ag BE.¹³

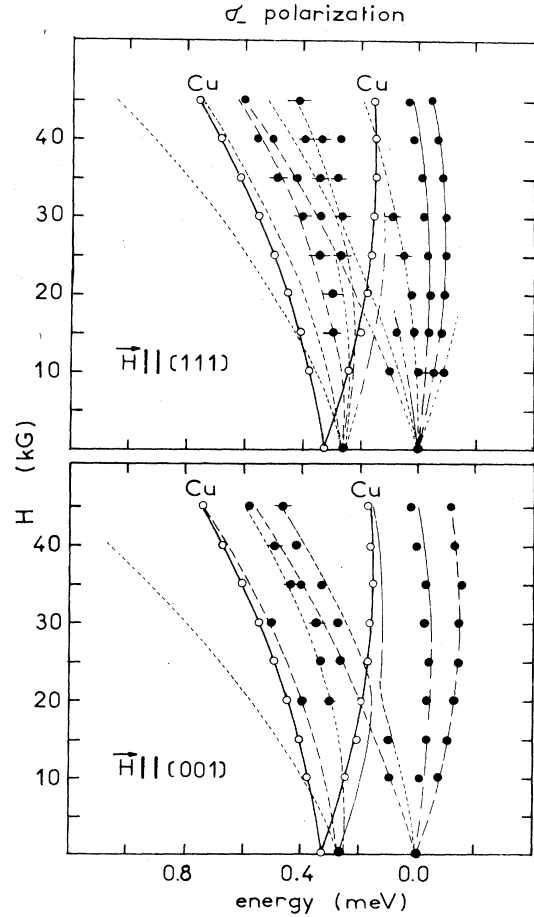
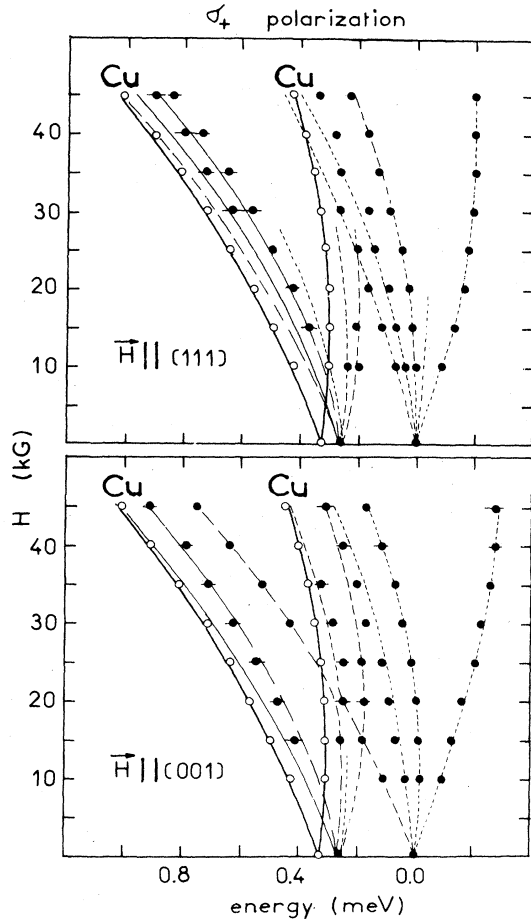


FIG. 8. Fan diagram showing the Zeeman effects observed for excitons bound to Cu (open circles) and Li (solid circles) in CdTe, for the σ_- polarization and $\mathbf{H} || \langle 100 \rangle$ and $\langle 111 \rangle$. The solid and dashed curves are the results of the calculations (see text).

FIG. 9. Same as in Fig. 8, but for σ_+ polarization.

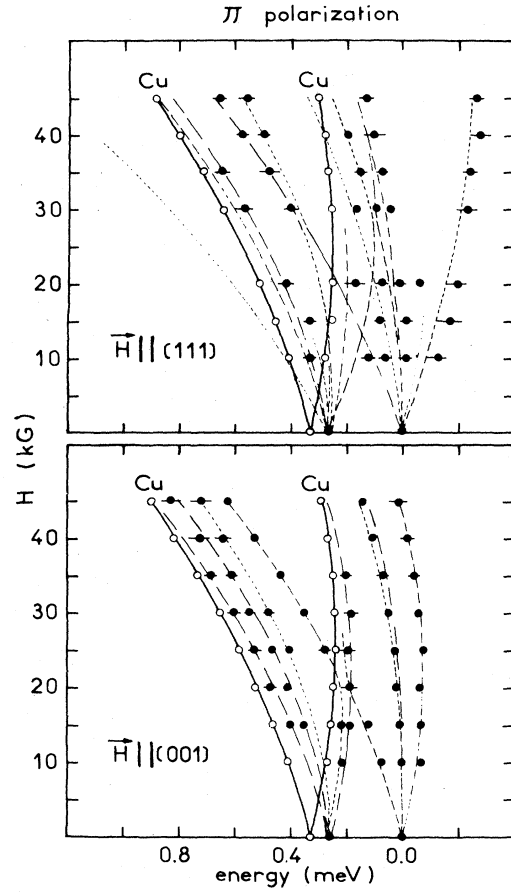
$$\begin{aligned} g_e &= -1.77, \\ K &= +0.61, \\ L &= -0.04. \end{aligned} \quad (6)$$

Thus the Zeeman effects have been calculated with only three adjustable parameters: b (electron-hole interaction), c (crystal-field term), and d (diamagnetic shift). The best fits to the data have been obtained for

$$\begin{aligned} b &= (-0.012 \pm 0.005) \text{ meV}, \\ c &= (-0.11 \pm 0.01) \text{ meV}, \\ d &= (1.6 \pm 0.1) \times 10^{-4} \text{ meV kG}^{-2}. \end{aligned} \quad (7)$$

Comparisons of calculations and experiments are shown in Figs. 8–10. The solid curves are the Zeeman splittings of the Cu BE lines calculated as in Ref. 13 but with a slightly smaller diamagnetic shift, $d = 1.32 \times 10^{-4} \text{ meV kG}^{-2}$. The dotted and dashed curves represent the calculations for the Li BE lines obtained by using the sets of parameter values (6) and (7) in Eqs. (3) and (5).

As expected, the fitting of the Li lines is more complex. We have not attempted to calculate the emission intensity of the transitions which depends on the oscillator strength and also on the population distribution within the BE

FIG. 10. Same as in Fig. 8, but for π polarization.

states. The determination of the population distribution requires a detailed analysis of the dynamics in a ten-level system. This is a delicate task, particularly when the recombination and relaxation rates are not well known. Instead, we calculate the oscillator strengths of all possible transitions for a given magnetic field direction and polarization (see the Appendix), and the results are normalized to 1. In the figures, transitions with oscillator strengths smaller than 0.1 are represented by the dotted curves, those with oscillator strengths larger than 0.8 are represented by the solid curves. The other cases are represented by the dashed curves, the dash length being approximately proportional to the oscillator strength. It can be seen that the oscillator strengths actually vary with the applied magnetic field due to interplays between the electron-hole interaction, the crystal-field term, and the Zeeman effect. As shown in the figures, the Zeeman splittings are very well reproduced for \mathbf{H} parallel to the $\langle 100 \rangle$ and $\langle 111 \rangle$ directions and for the three polarizations σ_+ , σ_- , and π .

The good agreement between the calculations and the experiments for either absorption (see Sec. IIIB) or PL in magnetic fields justifies the assumptions we have made above. It is interesting to note that the diamagnetic shift is about the same for exciton bound to Li, Na, Cu, and Ag acceptors. This effect is well explained in terms of the

pseudodonor model.⁹ In the model, the two holes of the acceptor BE are bound by the short-range potential of the acceptor. This in turn produces a long-range Coulomb potential which binds the excitonic electron in donorlike states. Therefore, the diamagnetic shift observed is that of the hydrogenic donor in CdTe.¹³

V. SUMMARY

We have investigated the fine structure of acceptor BE in CdTe. We have shown that (i) in the j - j coupling scheme, the level ordering of the $J=0$ and 2 two-hole states is inverted for deep- and shallow-acceptor BE, and (ii) the cubic-crystal-field effect is dominant over the electron-hole interaction. For Li and Na shallow acceptors, the low-lying BE states are derived from the $J=2$ two-hole state. The latter is first split by the cubic crystal field into a ground doublet Γ_3 and an excited triplet Γ_5 . Then interaction with the excitonic Γ_6 electron yields the sequence of Γ_8 ($K=\frac{3}{2}$), Γ_7 ($K=\frac{1}{2}$), and Γ_8 ($K=\frac{3}{2}$) BE states in order of increasing energy. The A_1^i ($i=\text{Li, Na}$) line has been assigned to the exciton recombination from the ground Γ_8 BE state and the A_{11}^i line to the exciton recombination from the excited and nearly degenerated Γ_7 and Γ_8 BE states. The Γ_6 ($K=\frac{1}{2}$) BE state deriving from the $J=0$ two-hole state has not been observed in the present work. For Cu and Ag deeper acceptors, the level ordering of BE states is just inverted. Thus the BE ground state is the Γ_6 ($K=\frac{1}{2}$) state which corresponds to the A_1^i ($j=\text{Cu, Ag}$) line. The broader line A_{11}^i at higher energy has been tentatively identified as due to unresolved Γ_8 ($K=\frac{3}{2}$), Γ_7 ($K=\frac{1}{2}$), and Γ_8 ($K=\frac{3}{2}$) BE states. The above assignment has provided a satisfactory account of all magneto-optical data presented in this paper.

APPENDIX

In this appendix we examine (i) the matrix representation of the linear Zeeman effect in the $j=\frac{3}{2}$ acceptor state

and in the BE states, and (ii) the optical selection rules for an arbitrary orientation of the magnetic field.

1. Linear Zeeman effect

Let $Oxyz$ be the coordinate system corresponding to the three fourfold crystal axes. We take the set of basis function $|j=\frac{3}{2}, j_z\rangle$ for the acceptor, and the set of basis function $|J=2, J_z\rangle$ and $|J=0\rangle$ for the BE. The quantization axis is z .

The two-hole states $|J=2, J_z\rangle$ and $|J=0\rangle$ can be expressed in terms of the one-hole states $|j=\frac{3}{2}, j_z\rangle$:

$$\begin{aligned} |2, \pm 2\rangle &= \pm \frac{1}{\sqrt{2}} (|\pm \frac{3}{2}\rangle_1 |\pm \frac{1}{2}\rangle_2 - |\pm \frac{1}{2}\rangle_1 |\pm \frac{3}{2}\rangle_2), \\ |2, \pm 1\rangle &= \pm \frac{1}{\sqrt{2}} (|\pm \frac{3}{2}\rangle_1 |\mp \frac{1}{2}\rangle_2 - |\mp \frac{1}{2}\rangle_1 |\pm \frac{3}{2}\rangle_2), \end{aligned} \quad (\text{A1})$$

$$\begin{aligned} |2, 0\rangle &= \frac{1}{2} (|+\frac{3}{2}\rangle_1 |-\frac{3}{2}\rangle_2 - |-\frac{3}{2}\rangle_1 |+\frac{3}{2}\rangle_2 \\ &\quad + |+\frac{1}{2}\rangle_1 |-\frac{1}{2}\rangle_2 - |-\frac{1}{2}\rangle_1 |+\frac{1}{2}\rangle_2), \\ |0, 0\rangle &= \frac{1}{2} (|+\frac{3}{2}\rangle_1 |-\frac{3}{2}\rangle_2 - |-\frac{3}{2}\rangle_1 |+\frac{3}{2}\rangle_2 \\ &\quad - |+\frac{1}{2}\rangle_1 |-\frac{1}{2}\rangle_2 + |-\frac{1}{2}\rangle_1 |+\frac{1}{2}\rangle_2), \end{aligned}$$

where $|j_z\rangle_i = |j=\frac{3}{2}, j_z\rangle$ of the i th hole ($i=1, 2$).

The matrix representation of the linear Zeeman effect (5) in the acceptor basis $|j=\frac{3}{2}, j_z\rangle$ is well known:²⁷

$$H_A = \mu_B H \begin{vmatrix} |+\frac{3}{2}\rangle & |+\frac{1}{2}\rangle & |-\frac{1}{2}\rangle & |-\frac{3}{2}\rangle \\ rA & (p-iq)C & 0 & (p+iq)D \\ (p+iq)C & rB & (p-iq)E & 0 \\ 0 & (p+iq)E & -rB & (p-iq)C \\ (p-iq)D & 0 & (p+iq)C & -rA \end{vmatrix} \begin{matrix} |+\frac{3}{2}\rangle \\ |+\frac{1}{2}\rangle \\ |-\frac{1}{2}\rangle \\ |-\frac{3}{2}\rangle \end{matrix}, \quad (\text{A2})$$

$$A = \frac{3}{2}K + \frac{27}{8}L, \quad B = \frac{1}{2}K + \frac{1}{8}L, \quad C = \sqrt{3}(\frac{1}{2}K + \frac{7}{8}L), \quad D = \frac{3}{4}L, \quad E = K + \frac{5}{2}L,$$

$p = H_x/H = \sin\theta \cos\phi$, $q = H_y/H = \sin\theta \sin\phi$, $r = H_z/H = \cos\theta$. (θ, ϕ) are the polar and azimuthal angles of \mathbf{H} in the coordinate system $Oxyz$.

Making use of (A1) and (A2) one obtains the matrix representation of the linear Zeeman effect in the two-hole basis $|J=2, J_z\rangle$:

$$\mu_B H \begin{vmatrix} | +2 \rangle & | +1 \rangle & | 0 \rangle & | -1 \rangle & | -2 \rangle \\ \hline \frac{4}{\sqrt{3}} rC & (p-iq)E & 0 & -(p+iq)D & 0 \\ (p+iq)E & r(D+E) & \sqrt{2}(p-iq)C & 0 & -(p+iq)D \\ 0 & \sqrt{2}(p+iq)C & 0 & \sqrt{2}(p-iq)C & 0 \\ -(p-iq)D & 0 & \sqrt{2}(p+iq)C & -r(D+E) & (p-iq)E \\ 0 & -(p-iq)D & 0 & (p+iq)E & -\frac{4}{\sqrt{3}} rC \end{vmatrix} \begin{matrix} | +2 \rangle \\ | +1 \rangle \\ | 0 \rangle \\ | -1 \rangle \\ | -2 \rangle \end{matrix} \quad (A3)$$

The Zeeman effect in the electron basis $|s = \frac{1}{2}, s_z\rangle$ is given by

$$\frac{1}{2} g_e \mu_B H \begin{vmatrix} | +\frac{1}{2} \rangle & | -\frac{1}{2} \rangle \\ \hline r & p-iq \\ p+iq & -r \end{vmatrix} \begin{matrix} | +\frac{1}{2} \rangle \\ | -\frac{1}{2} \rangle \end{matrix} \quad (A4)$$

(A4) is also the matrix representation of the linear Zeeman effect in the BE states $|J=0\rangle |s = \frac{1}{2}, s_z\rangle$. From (A3) and (A4) it is straightforward to get the matrix representation of the linear Zeeman effect [Eq. (4)] in the BE states $|J=2, J_z\rangle |s = \frac{1}{2}, s_z\rangle$.

2. Optical selection rules

We consider electric dipole transition from the initial state $|i\rangle$ to the final state $|f\rangle$. Its transition probability is proportional to $|\langle f | \mathbf{e} \cdot \mathbf{p} | i \rangle|^2$ where \mathbf{e} is the unit vector in the direction of the electric field polarization, and \mathbf{p} is the dipole moment operator. In practice, the light polarizations are defined with respect to the direction of the applied perturbation (magnetic field, uniaxial stress, etc.). Let $Ox'y'z'$ be the "polarization" coordinate system, with Oz' in the direction of the external magnetic field \mathbf{H} , for example. In this polarization coordinate system, we define the linear polarization π and circular polarizations σ_+ and σ_- ,

$$\mathbf{e}'_\pi = \mathbf{e}'_z, \quad (A5)$$

$$\mathbf{e}'_\pm = \mp \frac{1}{\sqrt{2}} (\mathbf{e}'_x \pm i \mathbf{e}'_y).$$

The unit vector \mathbf{e} can now be written

$$\mathbf{e} = u'_x \mathbf{e}'_x + u'_y \mathbf{e}'_y + u'_z \mathbf{e}'_z = u'_\pi \mathbf{e}'_\pi + u'_+ \mathbf{e}'_+ + u'_- \mathbf{e}'_- , \quad (A6)$$

with

$$u'_\pi = u'_z,$$

$$u'_\pm = \mp \frac{1}{\sqrt{2}} (u'_x \mp i u'_y).$$

Then it is easy to see that absorption (emission) selection rules for the polarization π , σ_+ , and σ_- are governed by the dipole moment operators P'_π (P'_π), P'_+ (P'_-), and P'_- (P'_+), respectively,

$$P'_\pi = P'_z,$$

(A7)

$$P'_\pm = \mp \frac{1}{\sqrt{2}} (P'_x \pm i P'_y).$$

Since the polarization coordinate system does not always coincide with the $Oxyz$ coordinate system chosen for the basis functions, we derive the relationships between the dipole moment operators defined in these two coordinate systems,

$$P'_\pi = \frac{\sin\theta}{\sqrt{2}} (-e^{-i\phi} P_+ + e^{i\phi} P_-) + \cos\theta P_\pi,$$

(A8)

$$P'_\pm = \frac{1 \pm \cos\theta}{2} e^{-i\phi} P_+ + \frac{1 \mp \cos\theta}{2} e^{i\phi} P_- \pm \frac{\sin\theta}{\sqrt{2}} P_\pi,$$

where (θ, ϕ) are the polar and azimuthal angles of \mathbf{H} in the $Oxyz$ coordinate system.

In this paper we are interested in exciton recombination from the initial BE states

$$|J_z; s_z\rangle \equiv |J=2, J_z\rangle |s = \frac{1}{2}, s_z\rangle$$

to the final acceptor states

$$|j_z\rangle \equiv |j = \frac{3}{2}, j_z\rangle.$$

The only nonzero matrix elements of dipole moment operators are the following:

π polarization

$$\langle \pm \frac{3}{2} | P_z | \pm 2; \mp \frac{1}{2} \rangle = -\frac{1}{\sqrt{3}},$$

$$\langle \pm \frac{3}{2} | P_z | \pm 1; \pm \frac{1}{2} \rangle = +\frac{1}{\sqrt{3}},$$

(A9)

$$\langle \pm \frac{1}{2} | P_z | 0; \pm \frac{1}{2} \rangle = +\frac{1}{\sqrt{6}}.$$

σ_+ and σ_- polarization

$$\langle \pm \frac{3}{2} | P_\mp | \pm 2; \pm \frac{1}{2} \rangle = -\frac{1}{\sqrt{6}},$$

$$\langle \pm \frac{1}{2} | P_\mp | \pm 2; \mp \frac{1}{2} \rangle = -\frac{1}{\sqrt{2}},$$

$$\langle \mp \frac{1}{2} | P_\mp | \pm 1; \mp \frac{1}{2} \rangle = -\frac{1}{\sqrt{2}},$$

$$\langle \mp \frac{1}{2} | P_{\mp} | 0; \pm \frac{1}{2} \rangle = + \frac{1}{\sqrt{12}},$$

$$\langle \mp \frac{3}{2} | P_{\mp} | \mp 1; \pm \frac{1}{2} \rangle = + \frac{1}{\sqrt{6}},$$

$$\langle \mp \frac{3}{2} | P_{\mp} | 0; \mp \frac{1}{2} \rangle = - \frac{1}{2},$$

The upper and lower signs correspond to the σ_+ and σ_- polarization, respectively.

For completeness, we give also matrix elements of transitions from the BE states $|0; s_z\rangle \equiv |J=0\rangle |s=\frac{1}{2}, s_z\rangle$ to the acceptor states $|j_z\rangle$:

π polarization

$$\langle \pm \frac{1}{2} | P_z | 0; \pm \frac{1}{2} \rangle = - \frac{1}{\sqrt{6}}.$$

σ_+ and σ_- polarizations

$$\langle \mp \frac{1}{2} | P_{\mp} | 0; \pm \frac{1}{2} \rangle = - \frac{1}{\sqrt{12}},$$

$$\langle \mp \frac{3}{2} | P_{\mp} | 0; \mp \frac{1}{2} \rangle = - \frac{1}{2}.$$

The upper and lower signs correspond to the σ_+ and σ_- polarizations, respectively.

*Present address: Centre d'Etudes Nucléaires de Grenoble, LETI/CRM 85X, 38041 Grenoble Cédex, France.

¹For a review, see P. J. Dean and D. C. Herbert, in *Excitons*, edited by K. Cho (Springer, Berlin, 1979), Chap. 3, p. 55.

²T. N. Morgan, *Proceedings of the 12th International Conference on the Physics of Semiconductors*, edited by M. H. Pilkun (Teubner, Stuttgart, 1974), p. 391.

³D. C. Herbert, J. Phys. C **10**, 3327 (1977).

⁴D. S. Pan, Solid State Commun. **37**, 375 (1981).

⁵B. Stébé and G. Munschy, Solid State Commun. **40**, 663 (1981).

⁶A. M. White, P. J. Dean, and B. Day, J. Phys. C **7**, 1400 (1974).

⁷M. Schmidt, T. N. Morgan, and W. Schairer, Phys. Rev. B **11**, 5002 (1975).

⁸H. Mathieu, J. Camassel, and F. Ben Chekroun, Phys. Rev. B **29**, 3438 (1984).

⁹W. Rühle and D. Bimberg, Phys. Rev. B **12**, 2382 (1975).

¹⁰W. Schairer, D. Bimberg, W. Kottler, K. Cho, and M. Schmidt, Phys. Rev. B **13**, 3452 (1976).

¹¹A. M. White, I. Hinchliffe, P. J. Dean, and P. D. Greene, Solid State Commun. **10**, 497 (1972).

¹²P. J. Dean, H. Venghaus, J. C. Pfister, B. Schaub, and J. Marine, J. Lumin. **16**, 363 (1978).

¹³E. Molva and Le Si Dang, Phys. Rev. B **27**, 6222 (1983).

¹⁴E. Molva, J. P. Chamonal, G. Milchberg, K. Saminadayar, B.

Pajot, and G. Neu, Solid State Commun. **44**, 351 (1982).

¹⁵E. Molva, J. P. Chamonal, and J. L. Pautrat, Phys. Status Solidi B **109**, 635 (1982).

¹⁶J. P. Chamonal, E. Molva, and J. L. Pautrat, Solid State Commun. **43**, 801 (1982).

¹⁷E. Molva, J. L. Pautrat, K. Saminadayar, G. Milchberg, and N. Magnea, Phys. Rev. B **30**, 3344 (1984).

¹⁸L. Svob and C. Grättepain, J. Solid State Chem. **20**, 297 (1977).

¹⁹A. M. White, P. J. Dean, L. I. Taylor, and R. C. Clarke, J. Phys. C **5**, L110 (1972).

²⁰P. Hiesinger, S. Suga, F. Willmann, and W. Dreybrodt, Phys. Status Solidi B **67**, 641 (1975).

²¹H. Venghaus and P. J. Dean, Phys. Rev. B **21**, 1596 (1980).

²²R. Romestain and N. Magnea, Solid State Commun. **22**, 1201 (1979).

²³A. Abragam and B. Bleaney, in *Electron Paramagnetic Resonance of Transition Ions* (Clarendon, Oxford, 1970), p. 665.

²⁴K. R. Elliott, G. C. Osbourn, D. L. Smith, and T. C. McGill, Phys. Rev. B **17**, 1808 (1978).

²⁵T. N. Morgan, J. Phys. C **10**, L131 (1977).

²⁶P. J. Dean and R. A. Faulkner, Phys. Rev. **185**, 1064 (1969).

²⁷A. Abragam and B. Bleaney, in *Electron Paramagnetic Resonance of Transition Ions* (Clarendon, Oxford, 1970), p. 721.